

Trends of boundary layer ozone pollution and VOC emissions in China as observed by OMI

Lu Shen

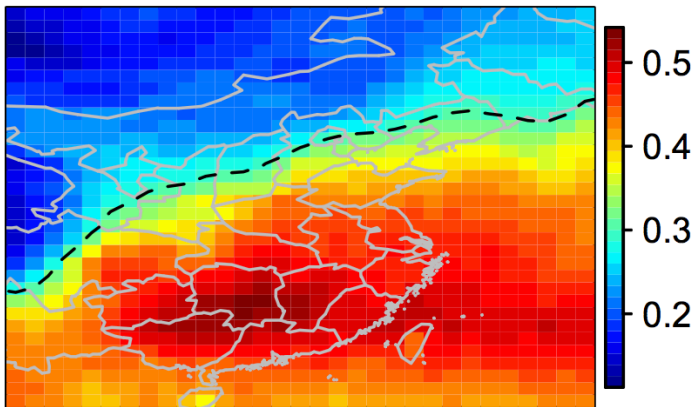
Harvard University

With Daniel Jacob, Xiong Liu, Guanyu Huang, Hong Liao, Ke Li, Lei Zhu, Qiang Zhang, Bo Zheng, and Melissa Sulprizio, Isabelle De Smede, Gonzalo González Abad, Hansen Cao, Tzung-May Fu

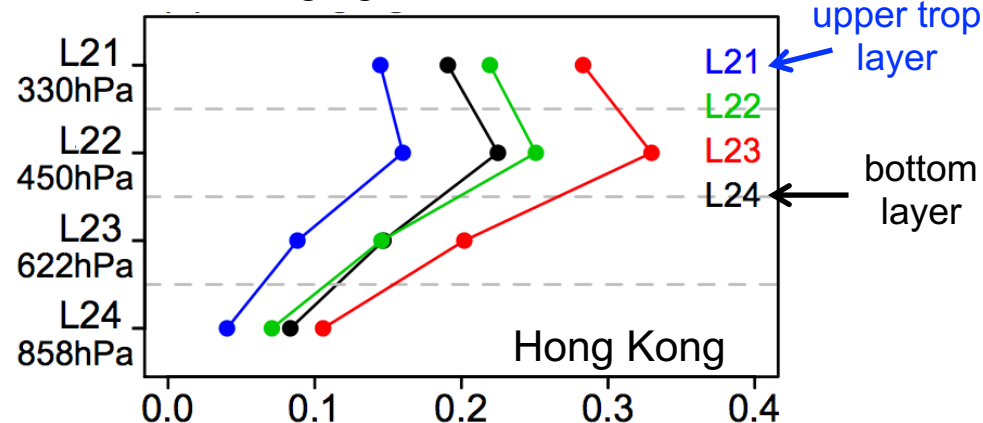
The OMI satellite instrument can capture spatial distribution of seasonal mean ozone in eastern China.

Data: We use the 2005-2017 OMI ozone profile retrieval (PROFOZ v0.9.03, level 2) product from the Smithsonian Astrophysical observatory (Liu et al, 2010).

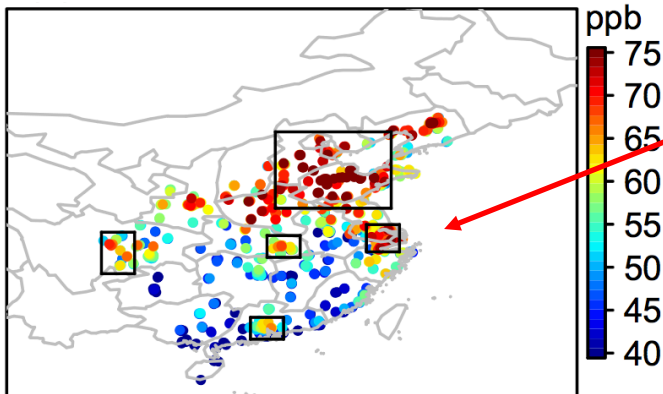
OMI DOFS below 400 hPa



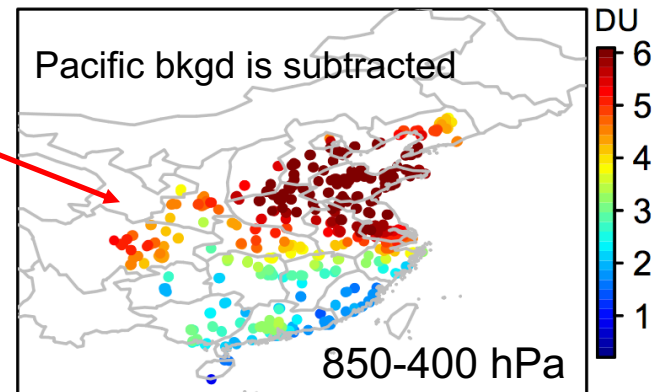
Averaging kernel sensitivities



Mean afternoon ozone, JJA 2013-2017

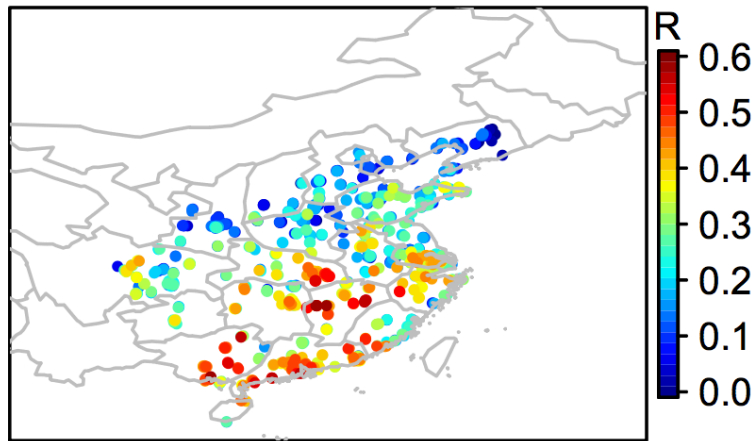


Mean OMI ozone enhancement



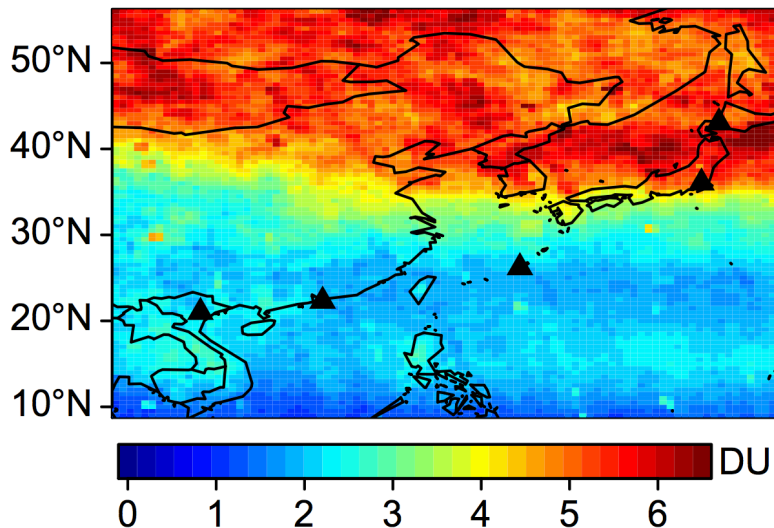
OMI can also capture the daily variability of boundary ozone in southern China.

Daily correlation, surface ozone vs.
OMI enhancements



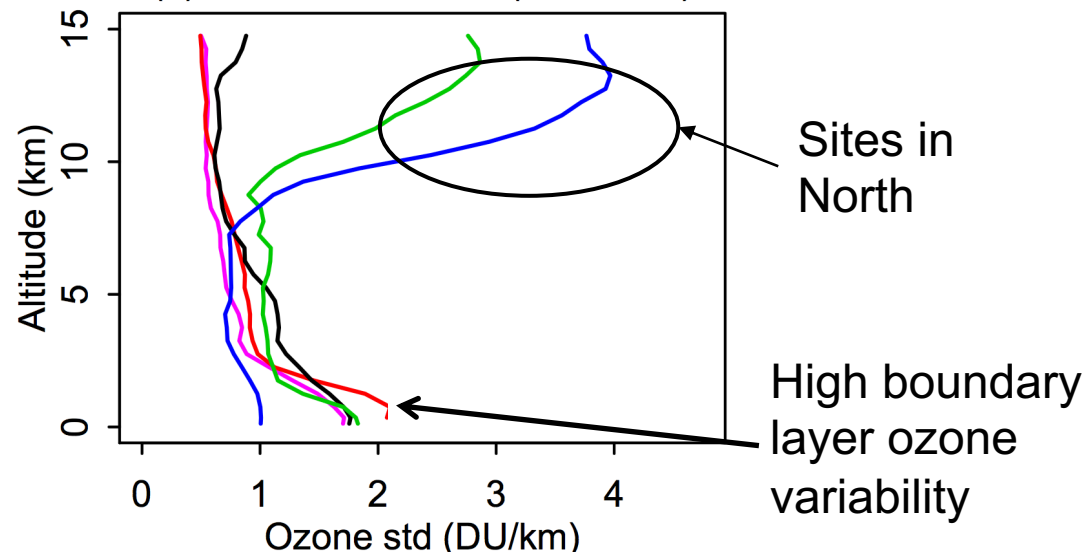
Standard deviation of ozone concentrations, summers 2005-2017

(a) OMI 400-200 hPa data



- Ozonesonde data show that much of the variability of OMI ozone over southern China in summer is driven by the boundary layer.
- We find much larger upper tropospheric ozone variability in the north, which is related to the location of jet wind and more active stratospheric influence.

(b) Ozonesonde data (1-km bins)

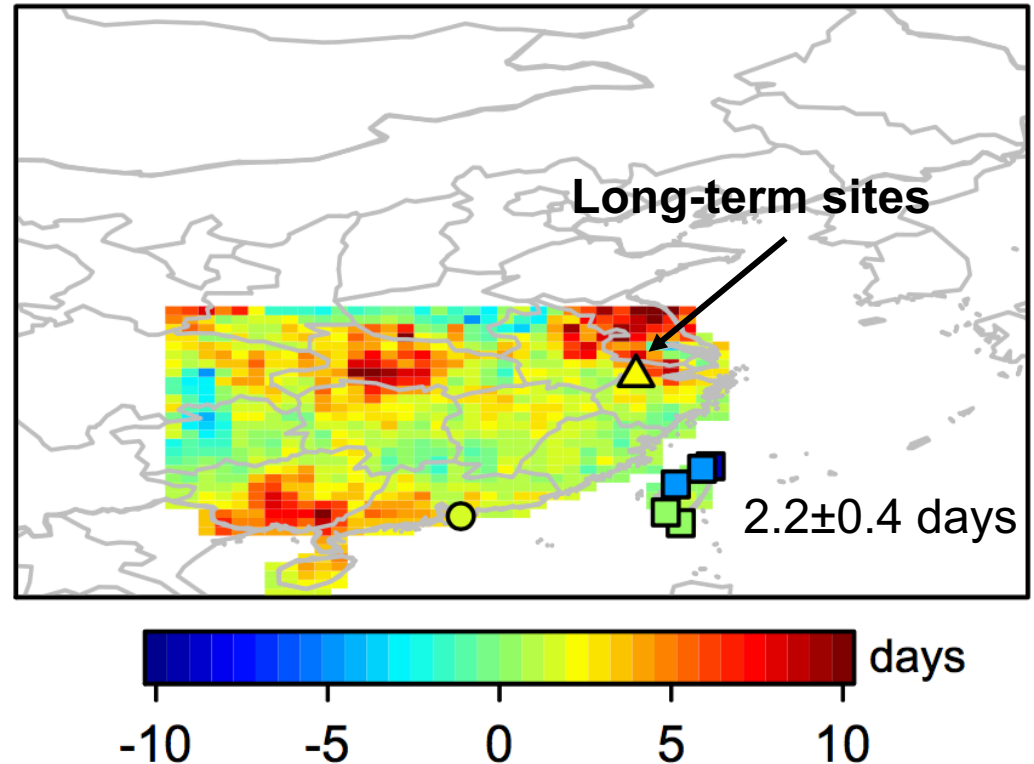


Changes in surface ozone pollution in China between 2005-2009 and 2013-2017

Changes of ozone episode days inferred from OMI
from 2005-2009 to 2013-2017

Method

We construct a point process model (Cole 2001) from the extreme value theory to estimate the likelihood of surface ozone episodes (>82 ppb) given the observed ozone enhancements.

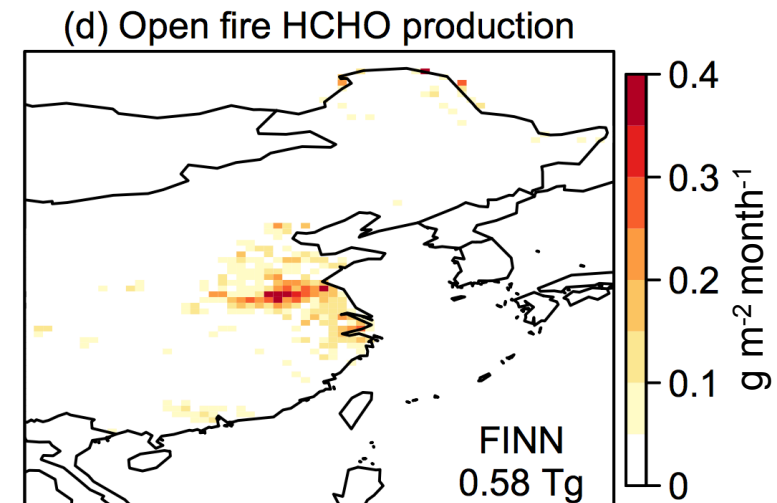
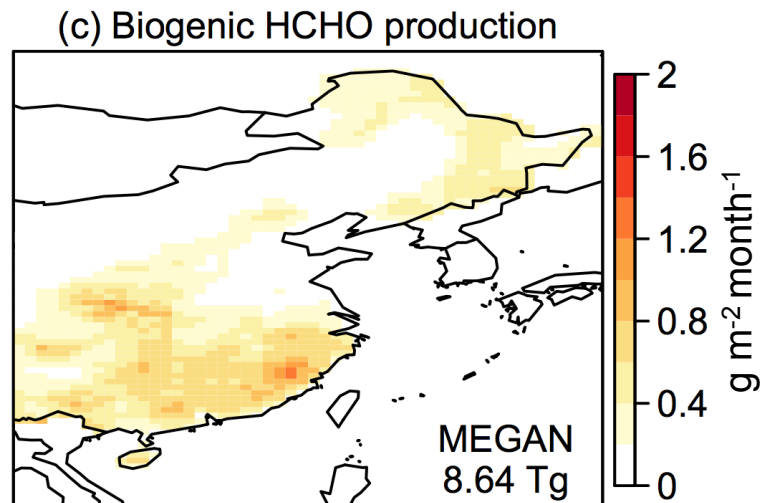
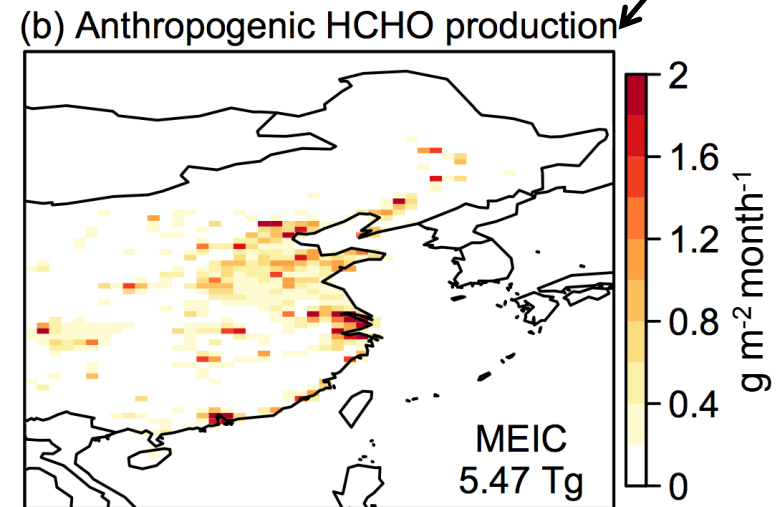
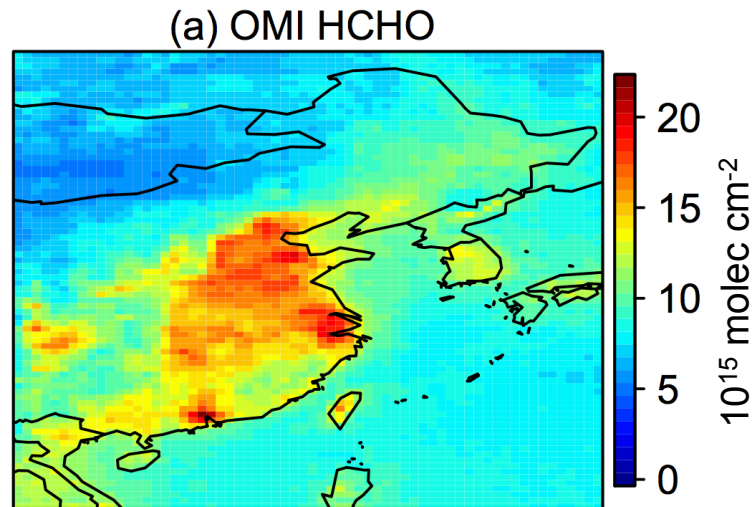


Ozone production in urban areas of China is thought to be VOC-limited. So we go on to examine VOC emission trends by using OMI formaldehyde (HCHO) as VOC proxy.

OMI HCHO column and HCHO production from different sources (May-September, 2005-2016)

Data: We use the 2005-2016 OMI HCHO product from the Smithsonian Astrophysical observatory (González Abad et al. 2015).

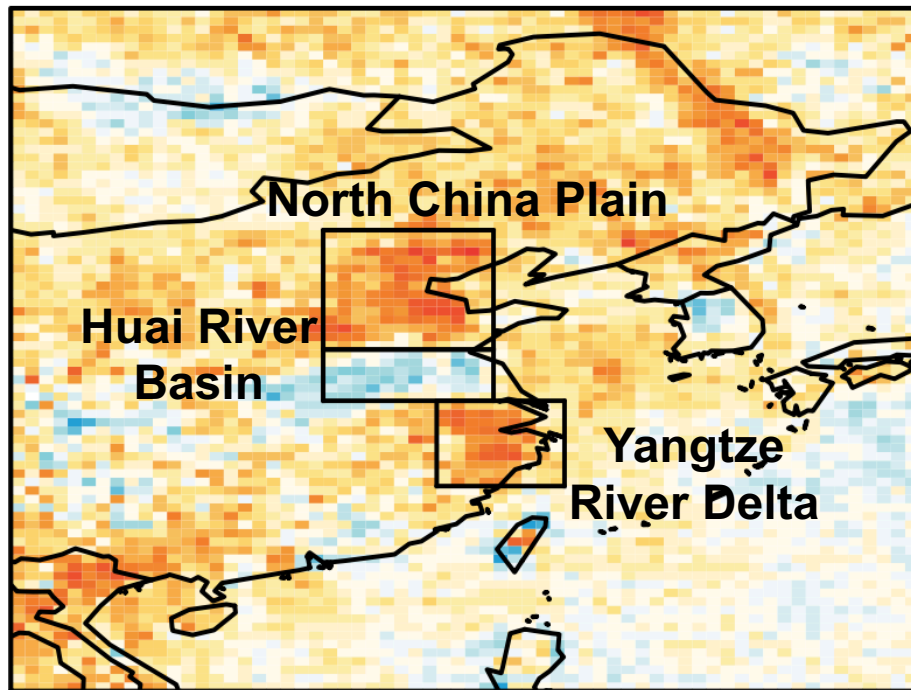
VOC x 1-day HCHO yields



OMI indicates increasing HCHO trends over much of eastern China, consistent with increasing anthropogenic VOC emissions.

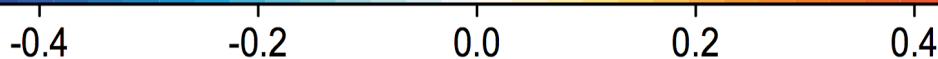
- We subtract a smoothed trend of HCHO column over the remote North Pacific.
- We subtract the linearly fitted temperature dependency to remove the effects of biogenic sources (Zhu et al., 2017).

May-September trends of HCHO columns, 2005-2016



$[10^{15} \text{ molec cm}^{-2} \text{ a}^{-1}]$

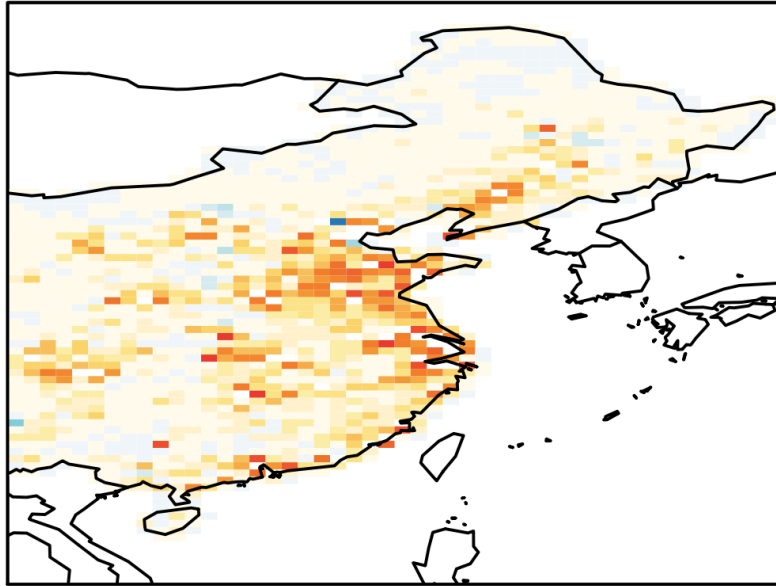
The OMI instrument shows large increases of HCHO columns in the North China Plain and the Yangtze River Delta region, consistent with the trend of anthropogenic VOC emissions.



The decreasing VOC emission in the Huai River Basin appear to reflect the bans on agricultural fires since the early 2010s

Linear trends of VOC emissions, 2005-2016

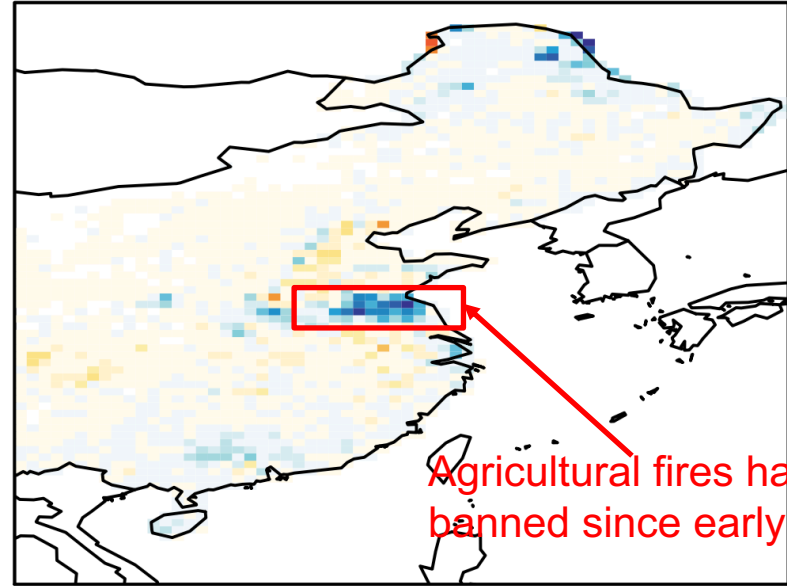
(a) Anthropogenic emissions (MEIC)



[g VOC m⁻² month⁻¹ a⁻¹]

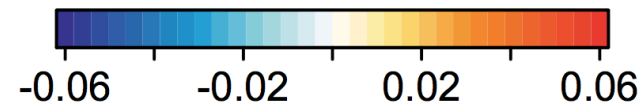


(b) Fire emissions (FINN)



Agricultural fires has been banned since early 2010s.

[g VOC m⁻² month⁻¹ a⁻¹]

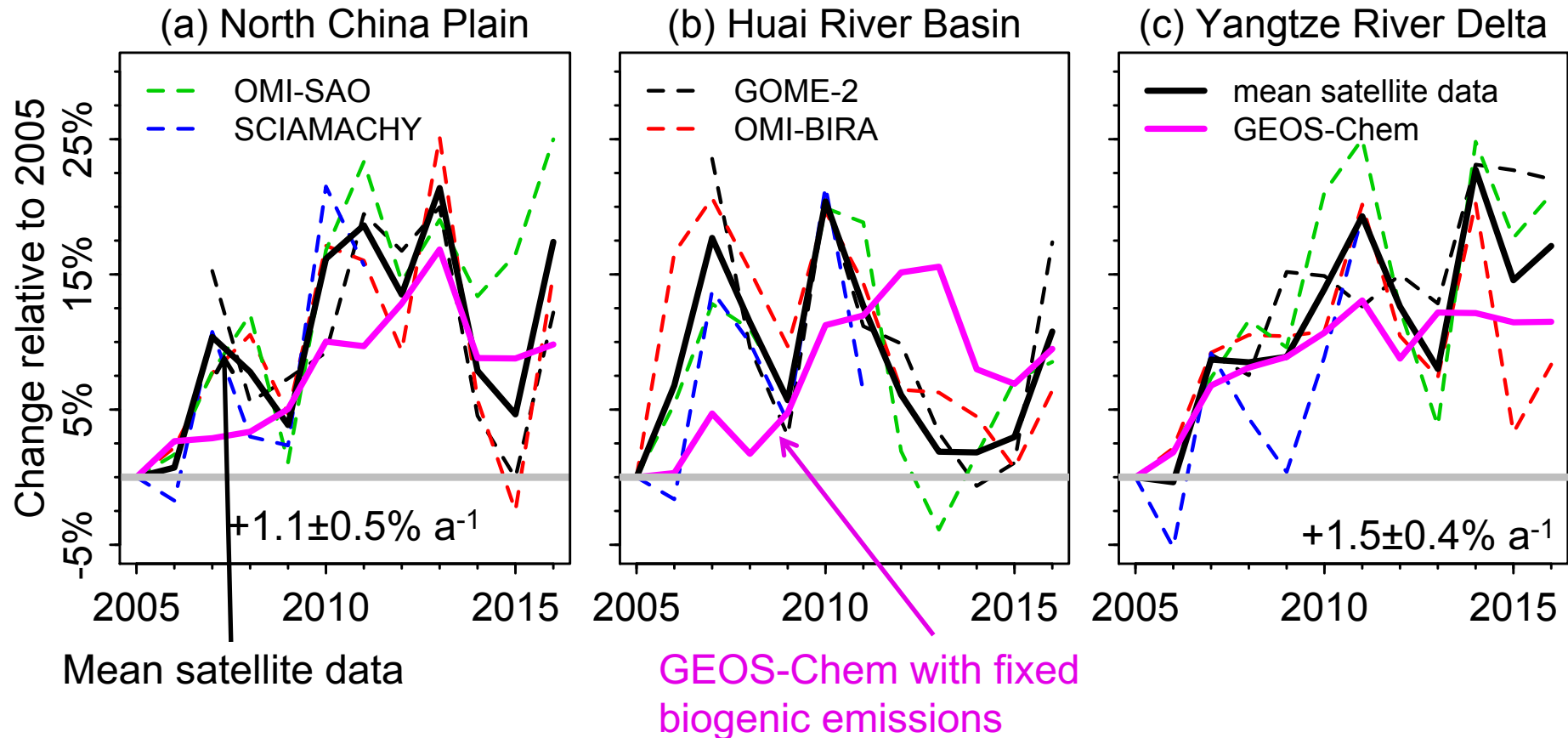


Color scales are different

Previous studies found that fire emissions here may be too low (e.g. Cao 2018; Stavrakou 2016)

2005-2016 timeseries of mean May-September HCHO columns from different satellite products

HCHO trends relative to 2005



- Different satellite products indicate generally consistent trends and variability.
- GEOS-Chem model can represent well the long-term trends in NCP and YRD using the bottom-up emission inventory.

Conclusions

- OMI can capture the mean summer spatial distribution of surface ozone over China, as well as the day-to-day variability (high-ozone episodes) in southern China.
- The 2005-2017 OMI record shows increasing frequency of high-ozone episodes in southern China.
- OMI formaldehyde observations show a large increase in anthropogenic VOC emissions in China over the 2005-2016 period, and a decrease in agricultural fire emissions since 2012.

HCHO production from anthropogenic and fire emissions in three representative regions.

The HCHO production rates are derived from the emissions of individual VOCs and 1-day HCHO yields of these VOC species from Chan Miller et al. (2016).

HCHO production from bottom-up anthropogenic (MEIC) and fire emissions (FINN)

